Biomaterials xxx (2014) 1–10

Contents lists available at ScienceDirect

Biomaterials

journal homepage: www.elsevier.com/locate/biomaterials

Differentiation of lung stem/progenitor cells into alveolar pneumocytes and induction of angiogenesis within a 3D gelatin – Microbubble scaffold

Thai-Yen Ling [a,b,*], Yen-Liang Liu [a,c], Yung-Kang Huang [a], Sing-Yi Gu [a,d], Hung-Kuan Chen [a], Choa-Chi Ho [e], Po-Nien Tsao [b,f], Yi-Chung Tung [g], Huei-Wen Chen [d], Chiung-Hsiang Cheng [h], Keng-Hui Lin [g,i], Feng-Huei Lin [c]

[a] Department of Pharmacology, College of Medicine, National Taiwan University, Taipei, Taiwan
[b] Research Center for Developmental Biology and Regenerative Medicine, National Taiwan University, Taipei, Taiwan
[c] Institute of Biomedical Engineering, National Taiwan University, Taipei, Taiwan
[d] Graduate Institute of Toxicology, College of Medicine, National Taiwan University, Taipei, Taiwan
[e] Department of Internal Medicine, National Taiwan University Hospital, Taipei, Taiwan
[f] Division of Neonatology, Department of Pediatrics, National Taiwan University Hospital, Taipei, Taiwan
[g] Research Center for Applied Sciences, Academia Sinica, Taipei, Taiwan
[h] Department and Graduate Institute of Veterinary Medicine, National Taiwan University, Taipei, Taiwan
[i] Institute of Physics, Academia Sinica, Taipei, Taiwan

ARTICLE INFO

Article history:
Received 29 January 2014
Accepted 27 March 2014
Available online xxx

Keywords:
Alveoli
Angiogenesis
Lung stem/progenitor cells
Microbubble-scaffold
Pneumocytes

ABSTRACT

The inability to adequately vascularize tissues *in vitro* or *in vivo* is a major challenge in lung tissue engineering. A method that integrates stem cell research with 3D-scaffold engineering may provide a solution. We have successfully isolated mouse pulmonary stem/progenitor cells (mPSCs) by a two-step procedure and fabricated mPSC-compatible gelatin/microbubble-scaffolds using a 2-channel fluid jacket microfluidic device. We then integrated the cells and the scaffold to construct alveoli-like structures. The mPSCs expressed pro-angiogenic factors (e.g., b-FGF and VEGF) and induced angiogenesis *in vitro* in an endothelial cell tube formation assay. In addition, the mPSCs were able to proliferate along the inside of the scaffolds and differentiate into type-II and type-I pneumocytes The mPSC-seeded microbubble-scaffolds showed the potential for blood vessel formation in both a chick chorioallantoic membrane (CAM) assay and in experiments for subcutaneous implantation in severe combined immunodeficient (SCID) mice. Our results demonstrate that lung stem/progenitor cells together with gelatin microbubble-scaffolds promote angiogenesis as well as the differentiation of alveolar pneumocytes, resulting in an alveoli-like structure. These findings may help advance lung tissue engineering.

1. Introduction

For most patients with end-stage lung disease, organ transplantation is the only option [1]. Unfortunately, the number of donors is limited; and therefore the ability to construct artificial lungs *in vitro* by tissue engineering is a promising solution [2].

Tissue engineering research for the regeneration of basic lung structures, including proximal cartilaginous airways, distal bronchioles, and alveolar sacs, is ongoing [2]. To date, transplantation of tissue-engineered airways has been successful [3,4]; however, the construction of alveolar sacs remains a challenge due to the complexity of the structure. Alveolar sacs are the major components of lung, and are composed of millions of interconnected small and thin-walled units, alveoli, which form a spongy, honeycomb-like lattice [5]. The alveolus is made of extracellular matrix with an interior lining of type-II and type-I pneumocytes wrapped in a fine mesh of capillaries [5]. The interactions between pneumocytes and capillary endothelial cells are important for alveogenesis and maintaining gas exchange functions [6,7]. However, data regarding the coordination of pneumocytes differentiation and blood vessel formation in the field of tissue engineering are limited.

* Corresponding author. Institute of Pharmacology, College of Medicine, National Taiwan University, No.1, Jen-Ai Rd., Sec. 1, Taipei, Taiwan. Tel.: +886 2 23123456x88322; fax: +886 2 3393 6987.
E-mail addresses: tyling@ntu.edu.tw, tyling1111@gmail.com (T.-Y. Ling).

http://dx.doi.org/10.1016/j.biomaterials.2014.03.074
0142-9612/

In early studies, cells from different sources were applied to various extracellular matrices or synthetic polymer-derived scaffolds in an effort to construct pulmonary-like structures [8–12]. These studies provided some basic knowledge, such as the compatibility of biomaterials and available cell sources for lung tissue engineering, yet the regulation of angiogenesis was not fully addressed. Recently, a perfusion-decellularized protocol was used to produce an artificial lung [13–15]. In contrast to the earlier studies, this method used both the cells derived from lung tissues and endothelial cells to repopulate a decellularized lung scaffold. The re-seeded epithelial cells showed a highly organized parenchymal structure and the re-seeded endothelial cells repopulated the vascular compartment within the acellular scaffold. Despite this success, little information was generated regarding the interactions between blood vessels and epithelial cells during alveolar development. In fact, the lack of adequate vascularization has dramatically hindered the progress of tissue engineering [16]. Therefore, elucidating the regulation of angiogenesis in order to provide an effective strategy for forming blood vessels during alveogenesis has remained a major goal in the field of tissue engineering.

Although there are different types of lung stem cells, their use in tissue engineering studies has been limited by their scarcity [17–21]. In previous studies, Ling et al. identified a rare population of pulmonary stem/progenitor cells from neonatal mouse lung tissue [22]. These mouse pulmonary stem/progenitor cells (mPSCs) preferred to grow on thin films of type-I collagen on polystyrene (PS)-based surface culture plates, and exhibited the self-renewal property of being able to form epithelial colonies of varying size with a surrounding stromal cells under chemically defined, serum-free primary co-culture conditions [22,23]. Additionally, the mPSCs were able to differentiate into alveolar type-II and type-I pneumocytes in sequential order [22].

Here, we plan to generate alveoli-like structures using mPSCs and microbubble-scaffolds which had been used for cartilage regeneration successfully [24]. We hypothesized that mPSCs may also have the pro-angionenic potential as well as the differentiation potential, and the microbubble-scaffolds will provide a microenvironment for mPSCs to differentiate into pneumocytes and to recruit blood vessel formation. To achieve the goal, we will identify a reliable cell surface marker to isolate enough cell number of mPSC for the study. In addition to endothelial tube formation assays, the other two experiments, an *in ovo* chicken chorioallantoic membrane (CAM) assay and subcutaneous transplantation of SCID mice, will be used to demonstrate the angiogenic potential of mPSCs-cellularized scaffold [25]. The outcomes for the application of mPSCs and microbubble-scaffolds may advance the progress of lung tissue engineering for inducing angiogenesis and pneumocytes differentiation in alveogenesis.

2. Materials and methods

2.1. Serum-free primary cell culture of mouse lung cells

The primary cell culture was performed as described previously [22]. Detailed methods are described in Supplementary Protocol S1.

2.2. Cytokine array analysis

Conditioned media derived from the mouse (lung tissue) primary culture (CM/mPC) at different time points (days 5, 10 and 14) were analyzed using Mouse_Cytokine_Array_C1000 (AAM-CYT-1000–8, RayBiotech, Norcross, GA) according to the manufacturer's instructions. Briefly, cytokine array membranes were blocked in 2 ml blocking buffer for 30 min and then incubated with the CM/mPC at room temperature for 2 h. After washing, membranes were incubated in diluted biotin-conjugated primary antibodies (1:200) at 4 °C overnight, followed by incubation in 1:1000 diluted horseradish peroxidase-conjugated streptavidin for 1 h. Membranes were then washed thoroughly and exposed to a peroxidase substrate for 2 min. Membranes were exposed to X-ray film (Kodak X-OMAT AR film) within 5 min of exposure to the substrate. Biotin-conjugated immunoglobulin G served as a positive control and the results were normalized for intensity.

2.3. Flow cytometry analysis and isolation of coxsackievirus/adenovirus receptor (CAR) -positive cell population

Cell suspensions obtained from the primary culture were analyzed for CAR-positive cells by flow cytometry using a FACS-calibur (BD Bioscience, San Jose, CA). Briefly, 1×10^6 cells were incubated with anti-CAR polyclonal goat-IgG (AF2654, R&D Systems, Minneapolis, MN) for 1 h. After washing, the labeled cells were incubated with Alex488-conjugated donkey-anti-goat secondary antibody (705–545-003, Jackson ImmunoResearch, West Grove, PA) with 1% BSA/PBS, and analyzed by flow cytometer. Isotypic IgG (005–000-003, Jackson ImmunoResearch, West Grove, PA) and unstained cells served as negative controls. To isolate the CAR-positive cell population, the same combination of antibodies described above were used in a FACS-AriaII (BD Bioscience, San Jose, CA). Propidium iodide (1 μg/ml) (P3566, Invitrogen, Carlsbad, CA) was added to the cell suspension to exclude dead cells during sorting. Sorted cells were spun down by low speed centrifugation (1100 rpm for 5 min) and re-suspended for later use, including cell differentiation experiments and construction of a cellularized 3-D scaffold.

2.4. In vitro differentiation

The *in vitro* differentiation experiment was performed as described previously [22] with the modification of using an isolated CAR-positive cell population.

2.5. Immunofluorescence staining

Cells in primary culture were fixed and stained as described previously [22]. Briefly, cells were incubated at 4 °C with primary antibodies against the following antigens: CAR, Oct-4, Sox-2 and Nanog. The mPSC-derived differentiated cells were also fixed and stained as previously described [22]. Cells were incubated overnight with primary antibodies against surfactant protein-C (SPC) and aquaporin-5 (Aqp-5), washed, and then incubated for 1 h at room temperature with the appropriate secondary antibodies. Cells were counterstained with DAPI. The antibody concentrations used in this study are listed in Supplementary Table S1.

2.6. RNA isolation and reverse-transcription polymerase chain reaction (RT-PCR)

Cells from the primary cell co-culture condition were isolated by FACS-AriaII as described above. The mPSCs (CAR-positive population) and stromal cells were collected. Two mouse cell lines, SVEC4-10 (mouse axillary lymph node/vascular epithelial cells) and MLE-15 (murine distal respiratory epithelial cells representative of type-II pneumocytes), were use as controls (SVEC4-10 was purchased from American Type Culture Collection and MLE-15 was a kind gift from Po-Nien Tsao [National Taiwan University Hospital]). Total RNA was prepared with the RNeasy Micro Kit (Qiagen, Valencia, CA), and reverse transcription was carried out with random primers using the SuperScript first-strand synthesis system (11904018, Invitrogen, Carlsbad, CA) according to the manufacturer's instructions. For PCR, the forward and reverse primers are listed in Supplementary Table S2.

2.7. In vitro tube formation assay

The assay was performed as previously described [26]. Matrigel (356231, BD Bioscience, San Jose, CA) was used to coat culture plates according to the manufacturer's instructions. About 150 μl of thawed Matrigel was applied to each well of 24-multiwell plates and polymerized at 37 °C for 1 h. SVEC4-10 cells were maintained in M199 medium (11150067, Invitrogen, Carlsbad, CA) with 10% FBS. SVEC4-10 cells (10^4 cells/well) in 0.3 ml medium with 10% FBS were plated on the Matrigel substratum, and 0.3 ml CM/mPC versus control medium was added after the cells attached. Phase images were taken every 2 h, and after 12 h, the cells were stained with Calcein AM (C34852, Invitrogen, Carlsbad, CA) (4 μM in M199, 300 μl/well), and incubated for 30 min in a 37 °C, 5% CO_2 incubator. The stained cells were observed by fluorescence microscopy and the number of tube branching points per field was quantified using Image-J. Six fields under 200× magnification were randomly selected in a single well. The results are expressed as the mean and the standard deviation of the mean from at least three experiments.

2.8. Preparation of coated culture plates

Biomaterials and the coating densities used in this study are listed in Supplementary Table S3. Solutions were added on PS-based surface culture plates and air dried in a laminar hood at room temperature for 12 h to form a thin film on the culture plates. Calcium chloride (0.1 M) was used to cross-link alginate-coated plates. Chitosan-coated plates were neutralized with 0.1 N NaOH solution for 2 h and then thoroughly washed with sterile distilled water. Gelatin-coated plates were cross-linked with 1% glutaraldehyde (GA) in distilled water or with 2% genipin (GP) (078–03021, Wako, Japan) in 70% ethanol for 4 h. The plates were thoroughly washed with sterile distilled water, and then 0.5 M glycine was added for 8 h to block the surplus GA or GP. The collagen and hyaluronic acid coated plates did not need additional treatment. All plates were washed with sterilized PBS before use.

2.9. Viability, cytotoxicity and colony forming assays

A colorimetric assay using the cell proliferation reagent WST-1 (11–644-807–001, Roche, Germany) was used to evaluate cell viability on different materials. Cells

Please cite this article in press as: Ling T-Y, et al., Differentiation of lung stem/progenitor cells into alveolar pneumocytes and induction of angiogenesis within a 3D gelatin – Microbubble scaffold, Biomaterials (2014), http://dx.doi.org/10.1016/j.biomaterials.2014.03.074

from the primary culture were re-seeded at 5×10^3 cells/well in 96-well plates coated with different materials. The cultures continued incubating at 37 °C for 24, 72 or 120 h. The ready-to-use WST-1 reagent was added to the culture during the last 2 h at 37 °C and the absorbance at 405 nm was measured. The cytotoxic effect of the coated plates was evaluated with a lactate dehydrogenase (LDH) assay (CytoTox96®, Promega, Fitchburg, WI). Cells from the primary culture were re-seeded (1×10^4 cells/cm^2) and incubated in 24-well plates coated with different materials. The supernatant (50 μl/well) was collected for the LDH assay after 24, 72 or 120 h. After 30 min incubation with kit reagents at room temperature, LDH activity, as a measure for cytotoxicity, was determined by spectrophotometric absorbance at 490 nm. The colony formation capacity of different coated plates was also estimated using cells from the primary culture.

2.10. Fabrication of microbubble-scaffold

The preparation of the microbubble scaffold was performed as described previously [24]. Details are described in Supplementary Protocol S2.

2.11. Cellularization of gelatin/microbubble-scaffolds

Gelatin/microbubble-scaffolds were punched with a biopsy punch (Miltex® Disposable 33–38, Miltex, York, PA) to obtain cylinder-shaped scaffolds (3 mm depth × 6 mm diameter). CAR-positive mPSCs isolated by FASC-AriaII were injected into the scaffolds (1×10^6 cells per scaffold) and the cellularized scaffolds were then cultivated in supplemented MCDB-201 culture medium in 6-well culture plates at 37 °C, 5% CO_2. After 4–5 days in culture, the cellularized scaffolds were used in *in vivo* angiogenesis assays, using either a chick embryo CAM assay or subcutaneous implantation in SCID mice [25]. For histological analysis, the cellularized scaffolds were incubated *in vitro* for another 7–9 days before staining as described in Section 2.15.

2.12. Chick embryo CAM assay and hemoglobin analysis

Fertilized Hisex brown chicken eggs were obtained from the Animal Health Research Institute (Danshui Dist., New Taipei City, Taiwan). Eggs were incubated under constant humidity at 37 °C. The CAM of a day 7 fertilized chick embryo was exposed by making a window in the egg shell, and an acellular- or mPSC-seeded gelatin/microbubble-scaffold was placed on top of the CAM for each egg. (The cellularized gelatin/microbubble-scaffolds had been cultivated for 7–9 days. Acellular scaffolds, which served as controls for this angiogenesis assay, were also cultivated for 7–9 days before implantation). After implantation, the window was sealed, and the eggs were incubated again. After 9 days of incubation, the implants were collected for whole-mount photography and for histological analysis, which was performed as described in Section 2.15.

To quantify angiogenesis in the scaffolds, the implants were collected, homogenized in PBS, and analyzed for hemoglobin [27]. The homogenate was mixed with 90% glacial acetic acid at a ratio of 1:9 for 20 min. The sample was centrifuged and the supernatant was collected for hemoglobin analysis. The standard Sigma–Aldrich method for measuring hemoglobin was modified for 96-well microtiter plates. Hemoglobin was assayed in triplicate by mixing 25 μl of homogenate with 100 μl of 3,3′, 5,5′- tetramethyl-benzidine–acetic acid solution (T2885, Sigma–Aldrich, St. Louis, MO). After adding 100 μl of 0.3% H_2O_2 solution and incubating at room temperature for 5 min, absorbance was read at 600–630 nm. Mouse hemoglobin (H2500, Sigma–Aldrich, St. Louis, MO) was used as a standard reference, and the data were analyzed with the Student's t test with $P < 0.05$ as significant.

2.13. Vascularization of the subcutaneous implants in SCID mice

Twenty-four C.B17/ICR-severe combined immunodeficient (SCID) mice (male, 4 weeks old, weight: 18.5 ± 1.3 g) obtained from the Laboratory Animal Center of College of Medicine, National Taiwan University, were used as recipients. Animals were maintained in accordance with the Guide for the Care and Use of Laboratory Animals, and the experimental protocols and surgical procedures were approved by the Institutional Animal Care and Use Committee. The operation was done under general anesthesia via intraperitoneum Ketamine injection. After adequate skin preparation and sterilization, an 8–10 mm incision was made in the skin of the back of the mouse to create a subcutaneous pocket. Cellularized gelatin/microbubble-scaffolds ($n = 6$ for each time point) or acellular scaffolds ($n = 6$ for each time point) were implanted into these subcutaneous pockets. For analysis of vascularization, FITC-conjugated dextran (FITC-dextran; Sigma–Aldrich, 5% (w/v) in PBS) was injected into the tail vein at day 7, 14 or 28 [28]. After injection for 10 min, the mice were sacrificed and the implants were removed and fixed in 4% formaldehyde/PBS for 2 h. The entire scaffold was analyzed by fluorescence microscopy for perfused blood vessels, which were visualized with FITC dextran. The implants were prepared for histological analysis as described in Section 2.15.

2.14. Scanning electron microscope (SEM)

The cellularized scaffolds from *in vitro* culture were fixed with 1% buffered glutaraldehyde solution for 2 h, washed in Ringer's solution, postfixed in cold 1% osmic acid, and dehydrated in graded alcohols. Afterward, scaffolds were critically point dried by Samdri-PVT-3B (Tousimis, Rockville, MD), and mounted on an aluminum stub. The scaffolds were then introduced into the chamber of the sputter coater (SPI, Sputter Coater, West Chester, PA) and coated with gold approximately 150 A thick. The specimens were studied with a JEOL JSM-6510LV type SEM (JEOL, Japan).

2.15. H&E staining and immunohistochemical staining

For histological or immunohistochemical analysis, the different constructions, including acellular gelatin/microbubble-scaffolds, cellularized scaffolds obtained from *in vitro* culture, cellularized and acellular scaffolds from the CAM angiogenesis assay, and the subcutaneous implants from SCID mice, were fixed in 10% formalin fixative, and embedded in paraffin. Afterward, 5 μm sections of lung tissue were obtained for hematoxylin and eosin (H&E) staining. Identification of SPC and Aqp-5 expression, antigen retrieval, and general immunohistochemical staining of paraffin-embedded sections of cellularized scaffolds were all performed as previously described [22]. Cells were incubated overnight with antibodies against SPC (Millipore, Billerica, MA) and Aqp-5 (Millipore, Billerica, MA), washed, and then incubated for 1 h at room temperature with FITC-conjugated goat anti-rabbit IgG secondary antibody (111–095-003, Jackson ImmunoResearch, West Grove, PA). Cells were counterstained with DAPI (D1306, Invitrogen, Carlsbad, CA). The concentrations of antibodies used in this study are listed in Supplementary Table S1.

2.16. Statistical analysis

Data are expressed as mean ± standard deviation. Statistical analyses of tube formation, cytotoxicity, cell viability, colony numbers and hemoglobin content were analyzed by ANOVA. If there were significant differences in these experiments by ANOVA, the Student's independent t-test was applied to analyze the differences between groups. Differences were considered significant if $P < 0.05$.

3. Results

3.1. The angiogenic potential of CAR-positive mPSCs

In general, tissue-specific stem cells are rare and heterogeneous in adult tissues, and their characterization has been limited due to technical difficulties. Recently, we identified a rare population of lung stem/progenitor cells (mPSCs) from neonatal mice [22,23]. These cells formed epithelial colonies with a surrounding stromal cells in a chemically defined serum-free medium (Fig. 1a–i and Supplementary Fig. S1-a), and expressed the stem cell markers Oct-4, Sox-2, and Nanog. (Supplementary Fig. S1-b) We identified a cell surface protein on mPSCs, coxsackievirus/adenovirus receptor (CAR), which was expressed at plasma membrane of mPSCs in the epithelial colonies (Fig. 1a-i and iii). Therefore, mPSCs were determined to represent a CAR-positive cell population, and as such, could be separated using flow cytometry (Fig. 1a-iv). The isolated cells showed the potential to differentiate into both type-II and type-I pneumocytic alveolar epithelial cells (Supplementary Fig. S2).

The chemically defined serum-free medium is free of serum-derived xenomaterials that may interfere with analyses. Therefore, the CM/mPC was analyzed, using a cytokine array, to reveal which cytokines and chemokines were expressed during co-culturing. As shown in Fig. 1b, the dot blots reveal that the pro-angiogenic factors VACM-1, b-FGF and VEGF were detected in the CM/mPC at days 3, 6, and 9 and were upregulated over time, while granulocyte colony-stimulating factor (G-CSF) was down-regulated. The ten cytokines with the highest expression levels at day 9 were identifed by quantification of intensities on the dot blots (Fig. 1c). To identify which cell type expressed these secreted pro-angiogenic factors, the isolated mPSCs and the CAR-negative stromal cell population were examined by RT-PCR. In the analysis, we used MLE15 cells, a mouse type-II pneumocyte cell line that has been reported to secrete VEGF [29]; and SVEC4-10 cells, a murine endothelium cell line, as positive controls [30]. As shown in Fig. 1d, mPSCs expressed pro-angiogenesis genes, including vascular cell adhesion molecule 1 (VCAM-1), b-FGF, and VEGF. Other pro-angiogenic cytokines (e.g., angiogenin, HGF and PDGF) which were not included in the array were also found to be expressed by mPSCs (Fig. 1d). Based on these results, we hypothesized that mPSCs have the potential to induce angiogenesis as well as to

Please cite this article in press as: Ling T-Y, et al., Differentiation of lung stem/progenitor cells into alveolar pneumocytes and induction of angiogenesis within a 3D gelatin – Microbubble scaffold, Biomaterials (2014), http://dx.doi.org/10.1016/j.biomaterials.2014.03.074

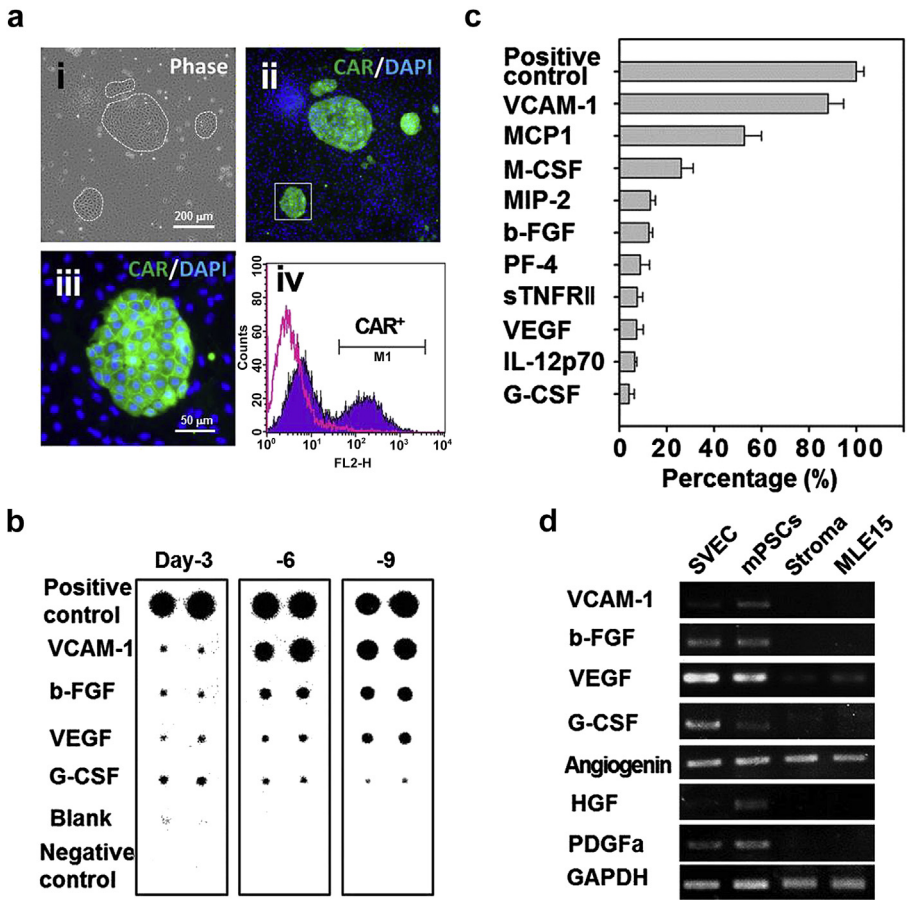

Fig. 1. Expression of pro-angiogenic factors by CAR-positive cells. (a-i) CAR-positive cells formed epithelial colonies of various sizes when co-cultured with stromal cells in a chemically defined, serum-free medium. In this phase image, the areas enclosed by white dotted lines indicate the epithelial colonies. (a-ii) Immunoflourescent image showing CAR staining at cell–cell junctions of the cells within the epithelial colonies. (a-iii) Magnification of the boxed area in panel a-ii. (a-iv) The CAR-positive population of the culture was identified and isolated by flow cytometry. (b, c) The cytokines secreted in the culture were analyzed using a cytokine array. The proangiogenic factors expressed in culture collected at days 3, 6, and 9 are indicated (e.g., b-FGF, VCAM-1 and VEGF). The expression of cytokines at day 14 were quantified by measuring the intensity of staining of cytokine array blot dots, and the10 cytokines with highest expression are shown. (d) RT-PCR analysis of the cells via flow cytometry isolation of the CAR-positive population of epithelial colonies. Pro-angiogenic factors, angiogenin, *HGF*, *b-FGF*, *G-CSF*, *PDGF*, *VCAM-1*, and *VEGF*, were analyzed. Lane 1, the SVEC4-10 cell line (mouse axillary lymph node/vascular epithelial cells); lane 2, CAR-positive population of mPSCs; lane 3, stromal cells; and lane 4, MLE-15 cell line (murine distal respiratory epithelial cell representative of type-II pneumocytes). *GAPDH* was used as an internal standard for both reactions.

differentiate into alveolar pneumocytes. To test this, we used an endothelial tube formation assay to test for angiogenetic potential. The mouse endothelial cell line SVEC4-10 was used in the assay to test for pro-angiogenic effects of CM/mPC. SVEC4-10 cells were seeded on Matrigel and incubated with the CM/mPC. As shown in Fig. 2a, SVEC4-10 cells formed capillary-like networks of tubes within 12 h of incubating in the CM/mPC. Quantification of the assay was performed by calcein AM staining and counting the number of branching points after 12 h. Significantly more branching points were seen after incubation with CM/mPC versus control medium (Fig. 2b and c). Taken together, these results suggest that mPSCs can induce angiogenesis.

3.2. Fabrication of microbubble-scaffolds by a 2-channel fluid jacket microfluidic device

To fabricate a scaffold that would mimic alveolar structure and support cell growth, biomaterials, such as alginate, chitosan, gelatin, gelatin cross-linked by genipin (gelatin/GP), gelatin cross-linked by glutaraldehyde (gelatin/GA), hyaluronic acid, and Type-I collagen from treated-PS/2D-surfaces were tested for cytotoxicity (LDH assay) and viability (WST assay). In addition, the ability to support colony formation, and the consistency and organization of the porous biomaterials were examined. As shown in Fig. 3a, alginate and chitosan showed high levels of cytotoxicity and were unable to support mPSC growth. Meanwhile, Type-I collagen, gelatin/GP and gelatin/GA demonstrated better abilities to support mPSC colony formation (Fig. 3b). Additionally, compared with Type-I collagen, both gelatin/GP and gelatin/GA formed highly organized scaffolds after gelation through a 2-channel fluid jacket microfluidic device (Fig. 3c-i). The gelatin-derived scaffolds were organized with interconnected and uniform pores arranged in a honeycomb pattern in each layer (Fig. 3c-i). For this study, we chose to use gelatin/GP to fabricate the microbubble-scaffolds because the gelatin/GA-derived microbubble-scaffolds showed strong green autofluorescence (data not shown). Slices obtained from paraffin-embedded gelatin/microbubble-scaffolds were prepared for H&E staining and then examined under microscopy. As seen in Fig. 3c-ii, the organization of the gelatin/microbubble-scaffold was similar to alveolar architecture and would be expected to provide an adequate physical environment for the mPSC.

3.3. Generation of an alveoli-like structure

To generate alveoli-like structures, CAR-positive mPSCs were seeded onto gelatin/microbubble-scaffolds (1×10^6 cells per

Please cite this article in press as: Ling T-Y, et al., Differentiation of lung stem/progenitor cells into alveolar pneumocytes and induction of angiogenesis within a 3D gelatin – Microbubble scaffold, Biomaterials (2014), http://dx.doi.org/10.1016/j.biomaterials.2014.03.074

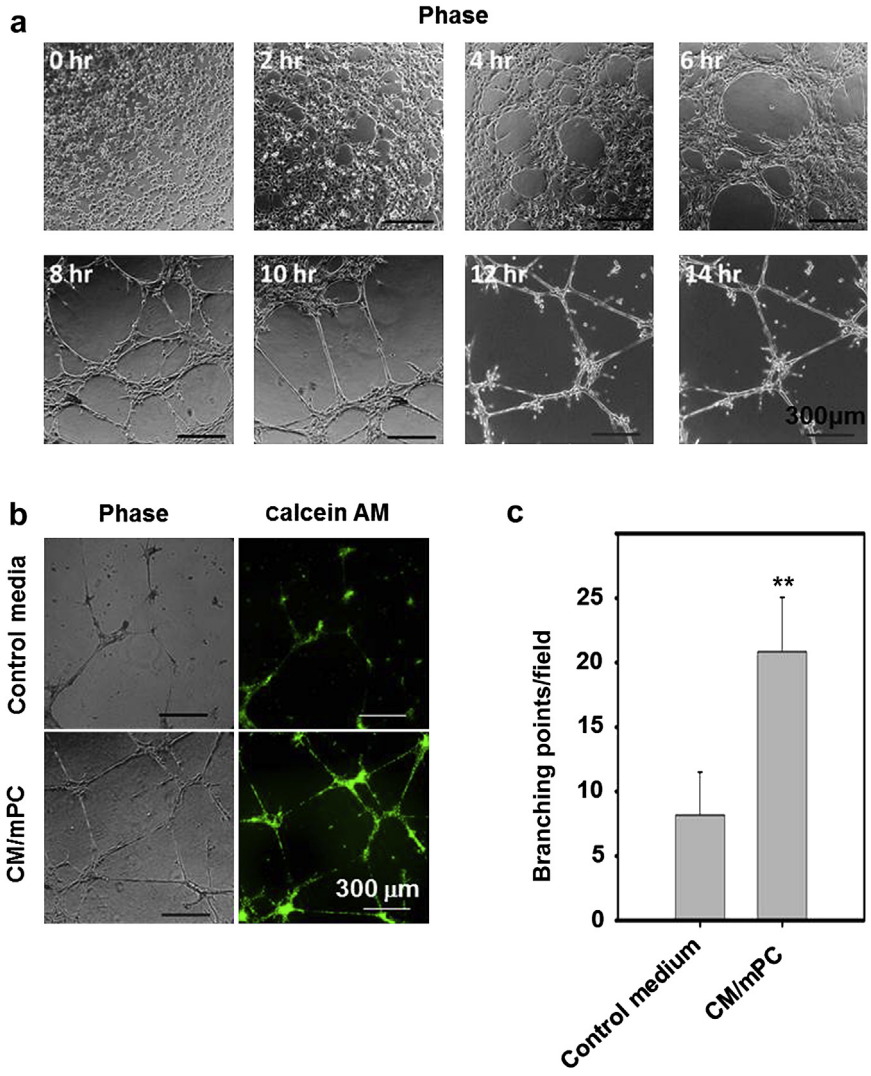

Fig. 2. Effect of conditioned medium derived from the primary culture on tube formation. (a, b) Tube formation assay. (a) SVEC4-10 cells were plated onto Matrigel-coated plates at a density of 1×10^4 cells per well and incubated in the presence of conditioned medium from the day-9 serum-free primary culture. MCDB-201 cell culture medium was used as a control. Phase images from different time points are shown. (b) At 12 h, changes in cell morphology were observed. Cells were stained with calcein-AM and photographed under fluorescent microscopy. (c) The area covered by the tube network was quantified by calculating branching points of SVEC4-10 cells using Image-Pro Plus software. Experiments were repeated three times. ($^{**}P < 0.01$, *t*-test). (CM/mPC: conditioned medium derived from the mouse lung primary culture).

scaffold) and then cultivated in medium for 7–10 days. As shown in Fig. 4, H&E staining of serial sections from paraffin-embedded scaffolds show that the mPSCs grew as a layer along the inside of the scaffold (Fig. 4a, arrows). An interconnected pore was also observed (Fig. 4a-iv, hollow arrowhead). The alignment of mPSCs on the inside of the scaffold was also demonstrated by SEM analysis (Fig. 4b). Furthermore, immunofluorescence staining indicated that the cells lining the inside of the scaffold expressed SPC (a cell marker for type-II pneumocytes) and Aqp-5 (a cell marker for type-I pneumocytes) (Fig. 4c). These results demonstrate that the gelatin microbubble-scaffold supports mPSC proliferation and differentiation into pneumocytes, which both contribute to make an alveoli-like structure.

3.4. Asssessment of angiogenesis in cellularized microbubble-scaffolds using a CAM assay

We initially utilized an *in ovo* method for assessing angiogenesis *in vivo* [25]. On day 3 of chick embryo development, a small window was made in the shell in order to detach the CAM layer from the egg shell. The window was resealed with adhesive tape and eggs were returned to the incubator until day 7 of chick embryo development. On day 7, gelatin/microbubble-scaffolds that had been cellularized in *in vitro* cultures, as well as acellular scaffolds, which were used as controls, were grafted on top of the CAMs ($n = 6$ chicken embryos for each type of scaffold). The chick embryos were then incubated with the scaffolds until day 14 of development. Whole-mounts of the scaffold grafts on day 14 are shown in Fig. 5a. Compared with the control (an acellular scaffold), the mPSC-containing gelatin/microbubble-scaffold had significantly more robust capillary network formation growing towards the implants (Fig. 5a). H&E staining of sections of paraffin-embedded scaffolds also showed more blood vessel formation in the cellularized gelatin/microbubble-scaffold than in the control scaffold (Fig. 5b). Quantitative analysis of the angiogenesis induced by the scaffolds was performed by determining the hemoglobin concentration of day 14 scaffold grafts (26). As shown in Fig. 5c, the cellularized gelatin/microbubble-scaffold had a significantly higher hemoglobin concentration than the acellular scaffold.

Please cite this article in press as: Ling T-Y, et al., Differentiation of lung stem/progenitor cells into alveolar pneumocytes and induction of angiogenesis within a 3D gelatin – Microbubble scaffold, Biomaterials (2014), http://dx.doi.org/10.1016/j.biomaterials.2014.03.074

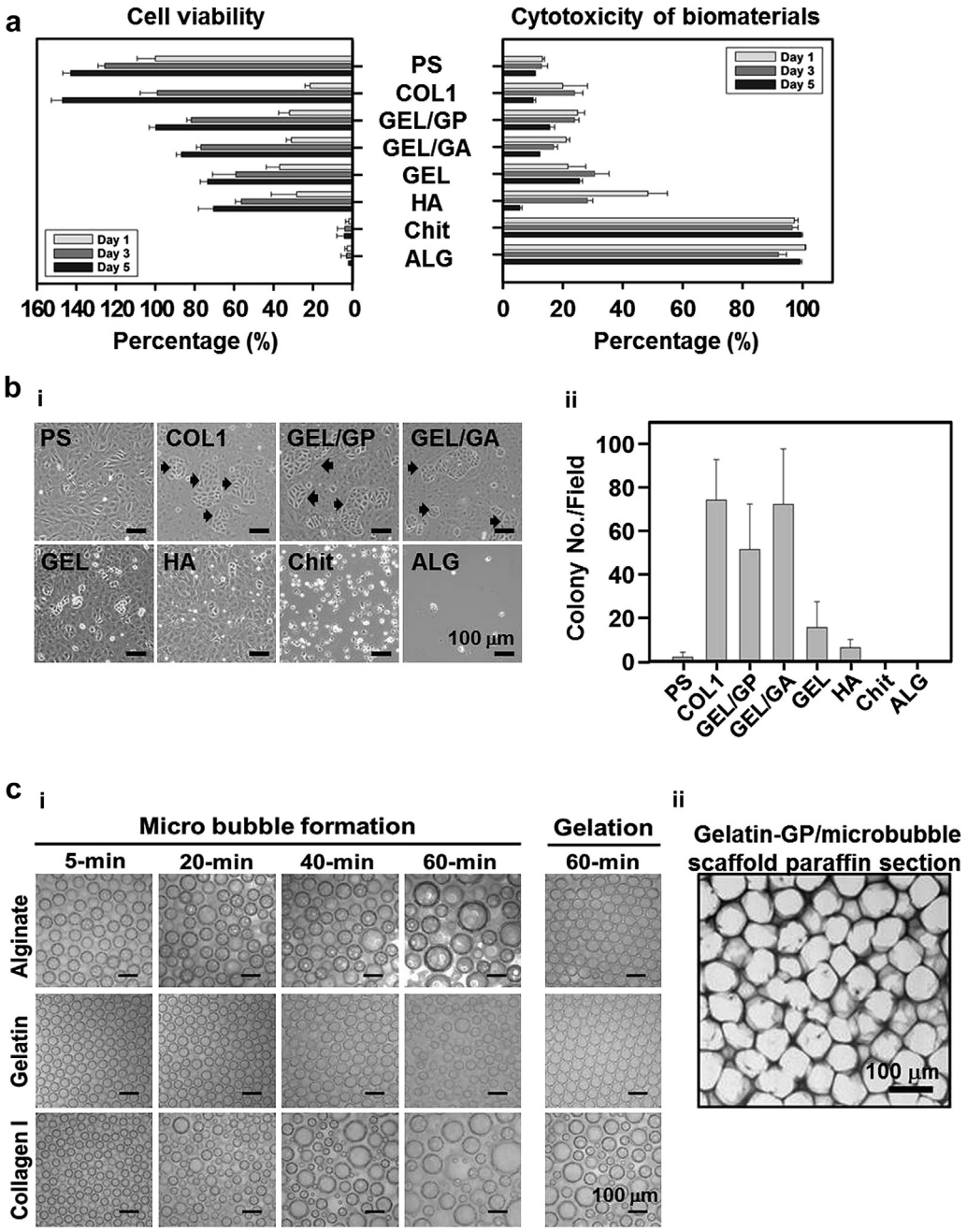

Fig. 3. Evaluation of different biomaterials for fabrication of microbubble-scaffolds. (a) Effect of different biomaterials on cell viability (WST assay) and toxicity (LDH assay) of mPSCs. Cells were incubated for 1, 3 and 5 days then cell viability was measured using a WST-1 assay and cytotoxicity was assessed using a LDH assay. Results are the mean ± sample standard deviation (SSD) of nine experiment for each group. PS: polystyrene-based surface culture plates (PS-culture plates); COL1: Collagen I-coated PS-culture plates; GE: Gelatin-coated; GEL/GP: Gelatin-coated & genapin-conjugated PS-culture plates; GEL/GA: Gelatin-coated & glutaraldehyde-conjugated PS-culture plates; HA: Hyaluronic acid-coated PS-culture plates; Chit: Chitosan-coated PS-culture plates; ALG: Alginate-coated PS-culture plates. (b) The ability of mPSCs to form epithelial colonies was examined by adding the primary cell culture to plates coated with various biomaterials and incubating for 7–9 days. (b-i) Arrows indicate the colonies formed by mPSCs. (b-ii) The number of re-formed mPSC colonies was quantified (×40 magnification, $n = 6$). Scale bar = 100 μm. (c) The self-assembly of mono-dispersed bubbles, created by the 2-channel fluid jacket microfluidic device, into microbubble foams is shown over 60 min. The resulting morphologies after gelation of alginate-, gelatin- and collagen-I-derived microbubble foams are shown. H&E staining of a section of paraffin-embedded gelatin/microbubble scaffold is shown. Scale bar = 100 μm.

3.5. Blood vessel formation in cellularized microbubble-scaffolds in SCID mice

In addition to the CAM angiogenic assay, we utilized SCID mice to examine the ability of microbubble-scaffolds to generate blood vessels. Cellularized gelatin/microbubble-scaffolds and control acellular scaffolds were subcutaneously implanted into the dorsal body cavities of SCID mice. Tail-vein injection of FITC-dextran was used to track blood vessel formation in the mice. Images of the FITC-dextran labeled blood vessel network were taken at days 7, 14, and 28. As shown in Fig. 6a-i, compared to the control scaffold (Fig. 6a-ii), day-28 cellularized gelatin/microbubble-scaffolds showed a marked increase of green fluorescence intensity. H&E staining of sections of paraffin-embedded scaffolds indicated that the cellularized section was covered by mPSC-derived cells, and the capillary network had thoroughly penetrated into the scaffold, in

Please cite this article in press as: Ling T-Y, et al., Differentiation of lung stem/progenitor cells into alveolar pneumocytes and induction of angiogenesis within a 3D gelatin – Microbubble scaffold, Biomaterials (2014), http://dx.doi.org/10.1016/j.biomaterials.2014.03.074

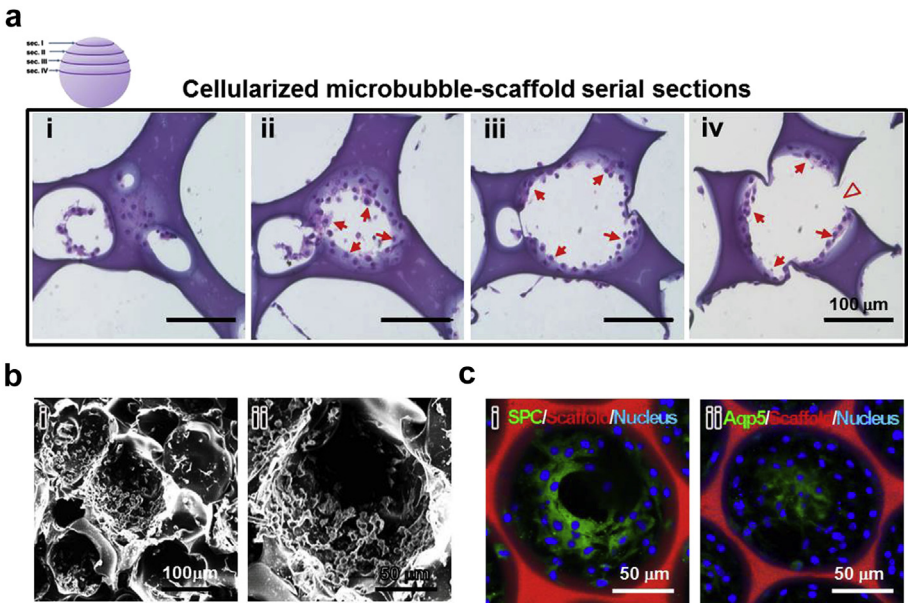

Fig. 4. *In vitro* cultivation of mPSCs in gelatin/microbubble-scaffolds. CAR-positive mPSCs (1×10^6) were seeded onto gelatin/microbubble-scaffolds and cultivated in medium for 7–9 days. (a) Figures a-i to a-iv show H&E staining of serial sections of the paraffin-embedded cellularized gelatin/microbubble-scaffold. Arrows indicate the growth of mPSCs on the inside of the microbubble-scaffold. The hollow arrowhead indicates the interconnected pore between the bubbles. Scale bar = 100 μm. (b-i & ii) SEM images of the cellularized gelatin/microbubble-scaffold. (c) On day 9, cells in the scaffold stained positive for both SPC protein (a marker of type-II pneumocytes) and Aqp-5 protein (a marker of type-I pneumocytes). Green, SPC or Aqp-5; Blue, DAPI; Red, scaffold intrinsic fluorescence. Scale bar = 50 μm.

contrast to the acellular scaffold at day 28 (Fig. 6b-i and ii and Supplementary Fig. S3). Again, positive immunostaining of SPC and Aqp-5 confirmed the presence of differentiated pneumocyte type-II cells (SPC) and type-I cells (Aqp-5) in the subcutaneous environment (Fig. 6c).

4. Discussion

Required components for construction of a complex organ include a cell source that can generate tissue-specific cell lineages, a strategy to induce angiogenesis, and compatible biomaterials to fabricate a 3D-scaffold [2,31]. Accordingly, Sugihara and co-workers first constructed an alveolus-like structure using a collagen gel matrix with isolated rat alveolar epithelial cells *in vitro* [8]. In subsequent studies, different cell sources were used with various biomaterials to mimic pulmonary-like structures [8–12]. Although some of these studies showed blood vessel formation by immunohistochemical staining [12], the information for regulation of angiogenesis was limited. Recently, Ott and colleagues used a perfusion-decellularized method with mixed population of rat fetal lung cells and human umbilical vein endothelial cells to generate artificial lungs [13]. Perterse et al. also used the method, and administered mixed populations of neonatal rat lung epithelial cells and microvascular lung endothelial cells to produce bio-artificial lungs [14]. Cotiella and co-workers utilized a decellularized lung as a scaffold for supporting murine embryonic stem cell differentiation to imitate lung tissues [15]. However, the interactions between blood vessels and the epithelium of the alveolar structure have not yet been fully addressed.

Different kinds of lung stem cells have been reported [17–21] but the use of these stem cells to generate artificial lungs is restricted. The scarcity of lung stem cells makes them unsuitable for tissue engineering [2]. In this study, we found that CAR expression was observed at the cell–cell junctions within mPSCs epithelial colonies in the culture, and was identified as one of the cell surface markers of mPSCs (Fig. 1a-ii &-iii). The receptor has been found in all normal organs, except in human brain [32]. In lung tissues, CAR is detected in the trachea and bronchi, but is absent from the alveoli of adult animals [33]. Therefore, mPSCs could be isolated and enriched by a two-steps procedure from the co-culture condition: a serum-free primary culture followed by FACS isolation for the CAR-positive population (Fig. 1a-iv). This procedure can serve as a stable source of mPSCs for further applications in tissue engineering, and avoids fluctuations caused by batch variability. The isolated cells could differentiate into alveolar pneumocytes *in vitro* (Supplementary Fig. S2).

By the serum-free primary culture, cytokines and growth factors expression in CM/mPC could be identified without interference from serum-derived xeno-materials. Cytokine array analysis indicated that VCAM-1, b-FGF, VEGF and G-CSF were identified in CM/mPC (Fig. 1b). Moreover, the other pro-angiogenic factors (e.g., platelet-derived growth factor-alpha, angiogenin and hepatocyte growth factor) whose antibodies-probes were not included in the cytokine array, were also positively identified for mPSCs expression by RT-PCR (Fig. 1d). The pro-angiogenic potential was further demonstrated *in vitro* with murine endothelial cells, SVEC4-10, in the tube formation assay (Fig. 2). Actually, angiogenesis is a complex process involving different cells and factors for stimulation, promotion, and stabilization of new blood vessels [34–36]. The mesenchymal cells have been suggested as a primary source of VEGF, which stimulates the vascular endothelium for capillary remodeling during lung development [37,38]. Lung fibroblasts have been reported to hold pro-angiogenic potential for immature capillary formation [38]. In acute injury, type-II pneumocytes have been reported to produce VEGF to protect alveolar epithelial cells from caspase-dependent apoptosis [39]. Our findings demonstrated that stromal cells could express VEGF and angiogenin, but mPSCs could express multiple pro-angiogenic factors. The results suggested that mPSCs played important roles in controlling the formation of blood vessels and capillary networks. For this reason, we hypothesized that mPSCs may display a dual-function: regulation of angiogenesis and differentiation into alveolar epithelial

Please cite this article in press as: Ling T-Y, et al., Differentiation of lung stem/progenitor cells into alveolar pneumocytes and induction of angiogenesis within a 3D gelatin – Microbubble scaffold, Biomaterials (2014), http://dx.doi.org/10.1016/j.biomaterials.2014.03.074

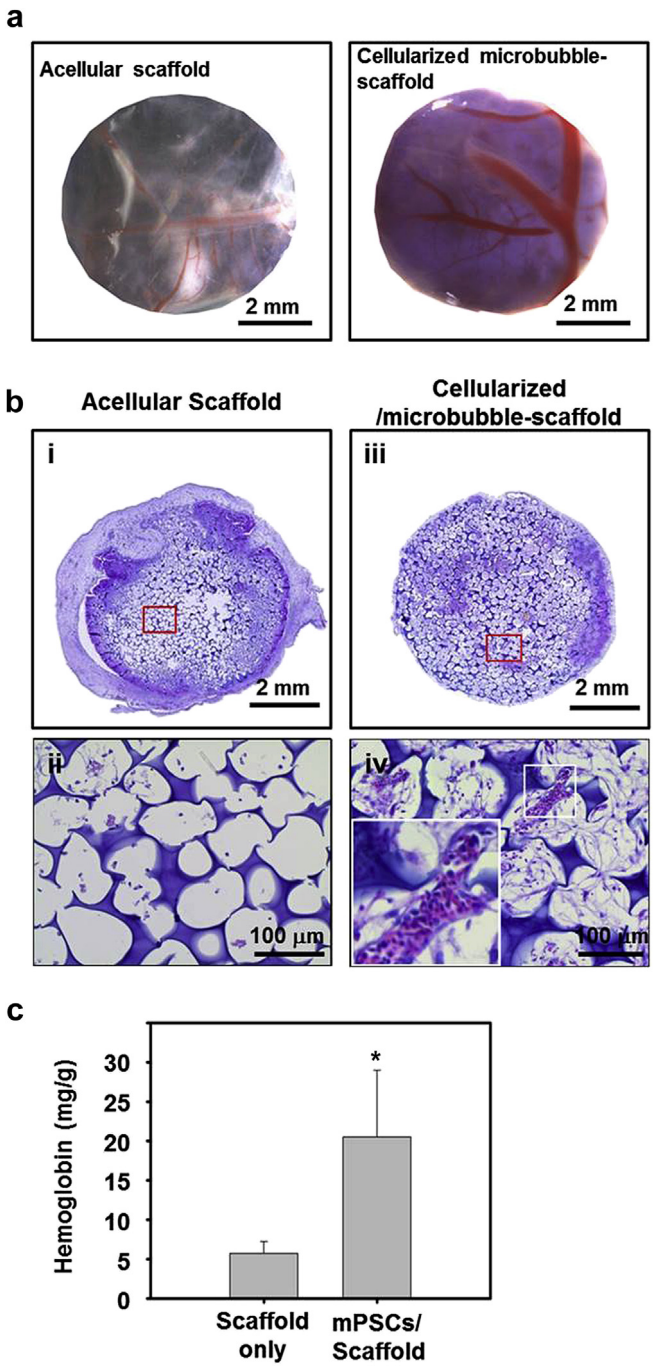

Fig. 5. *In ovo* angiogenesis of cellularized gelatin/microbubble-scaffolds. An i*n ovo* CAM assay was used to study angiogenesis. After 5 days in culture, the cellularized gelatin/microbubble-scaffolds and acellular scaffolds were individually implanted on the CAM. (a-i & ii) Whole-mount photographs of the implanted scaffolds after 7–8 days incubation are shown. Highly vascularized networks were observed in cellularized gelatin/microbubble-scaffolds. Scale bar = 2 mm (b) H&E staining of sections of paraffin-embedded scaffolds. (b-i & iii) Images show blood vessel formation in the cellularized scaffolds. (b-ii & iv) Magnified image of the red boxed areas in panels b-i and b-iii, respectively. In panel b-iv, inset shows magnification of the white boxed area, showing the pattern of blood vessels. (c) Quantification of hemoglobin concentration in cellularized gelatin/microbubble-scaffolds and acellular scaffolds. ($n = 3$, $^*P < 0.05$, *t*-test).

cells, which make mPSCs useful to apply for lung tissue engineering.

The positive results of mPSCs for pneumocytes differentiation and the endothelium tube formation led us to consider using a 3D-scaffold for mPSCs culture to demonstrate simultaneously for pneumocytes differentiation and blood vessel formation. Previous studies have shown that a 2-channel fluid jacket microfluidic device can construct highly organized alginate/microbubble-scaffolds [24,40]. These alginate/microbubble-scaffolds were successfully used for cartilage tissue engineering [24], but they could not support mPSCs growth (Fig. 3a and b). Stem cell proliferation and viability can be regulated by different biomaterials [41]. In addition, the CAR-positive mPSCs are adhesive cells that need cell matrix interactions to maintain their survival and growth. Alginate lacks the intrinsic motifs for cell adhesion that will lead to anoikis of transplanted cells. In other researches, modifications to alginate are made to provide cell–matrix interactions [42,43]. Thus, factors such as material topography and cytotoxicity must be evaluated. An ideal biomaterial should support both mPSCs viability and epithelial colony formation, and have the properties necessary to make a uniform microbubble-scaffold. Collagen-I could support mPSCs proliferation [22,23], however collagen-I couldn't form uniform porous scaffolds (Fig. 3c). After evaluation, the gelatin cross-linked by GA appeared to possess the most favorable properties and could assemble into a highly uniform microbubble-scaffold (Fig. 3c). Additionally, a previous study had demonstrated that the stiffness of these gelatin-derived scaffolds was 3–10 kPa [44], which is similar to that of normal alveolar wall (0.5–5 kPa) [45].

After scaffold construction, mPSCs was added to produce cellularized scaffold. H&E staining of serial sections of the paraffin-embedded cellularized scaffold showed the adherent cells expanding on the inner walls of the microbubble-scaffolds (Fig. 4a), and these cells stained positive for both type-II and type-I pneumocytes after 7–9 days in culture (Fig. 4c). These cellularized scaffolds not only had a porous consistency, but the multiple interconnections between the microbubbles of the scaffold resembled the pores of Kohn of lung alveoli [46]. All these features validate the choice of the gelatin/microbubble-scaffolds for studying mPSCs behaviors *in vitro*; however, the intrinsic red autofluorscence of the scaffold was a major defect to interfere with fluorescent microscopy.

The CAM assay was used first to test mPSCs-cellularized scaffolds the potential of blood vessel formation [25]. Macroscopic images of the scaffold showed significant neovascularization with capillary network formation after 7–9 days *in ovo* incubation after mPSCs-cellularized scaffolds were implanted (Fig. 5). Both the H&E staining of paraffin-embedded sections of the implants and the hemoglobin concentration analysis indicated that mPSCs-cellularized gelatin/microbubble-scaffolds could recruit blood vessel formation (Fig. 5b and c). Next, the angiogenic potential was evaluated by subcutaneously implanting mPSCs-cellularized scaffolds into the dorsal body cavity of adult SCID mice comparing with control acellular scaffolds. Fluorescence dye tracing and H&E staining of the scaffolds were used to analyze the formation of blood vessels. The acellular and cellularized implanted scaffolds were examined at different time points after injection of the FITC-dextran. As shown in Fig. 6a, an obvious increase in green fluorescence intensity, signifying blood vessel formation, was observed in the cellularized scaffolds between day 7 and day 28. The fluorescence intensity of cellularized scaffolds was much higher than the intensity of the control scaffold at day 28. H&E staining of paraffin-embedded scaffold sections also showed a higher density of blood vessels in mPSCs-cellularized scaffolds versus acellular scaffolds at day 28, and erythrocytes within the blood capillaries were observed throughout the scaffold (Fig. 6b & Supplementary Fig. S3). Meanwhile, positive immunostaining for SPC and Aqp-5 further confirmed the presence of differentiated type-II (SPC-positive) and type-I (Aqp-5-positive) pneumocytes in the scaffolds (Fig. 6c).

Please cite this article in press as: Ling T-Y, et al., Differentiation of lung stem/progenitor cells into alveolar pneumocytes and induction of angiogenesis within a 3D gelatin – Microbubble scaffold, Biomaterials (2014), http://dx.doi.org/10.1016/j.biomaterials.2014.03.074

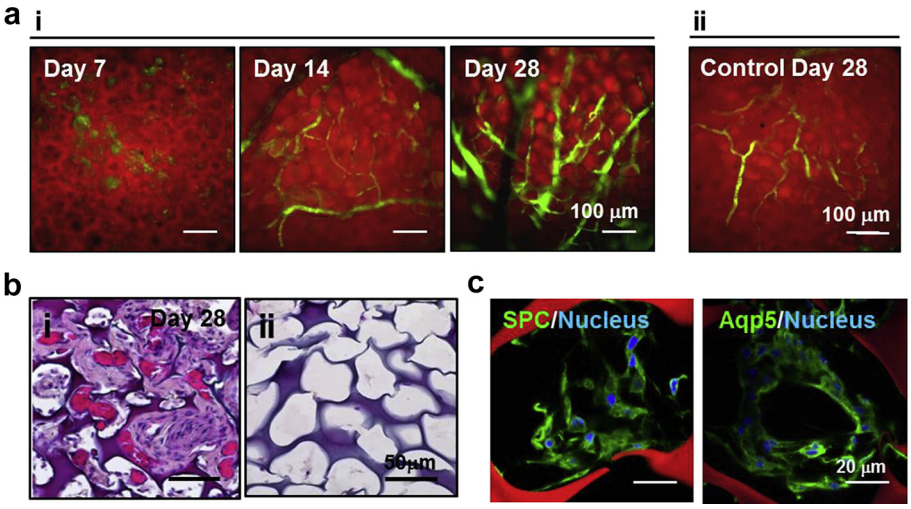

Fig. 6. *In vivo* angiogenesis of cellularized gelatin/microbubble-scaffolds after subcutaneous implantation in SCID mice. Cellularized gelatin/microbubble-scaffolds from *in vitro* culture and acellular scaffolds were implanted subcutaneously into the dorsal body cavity of adult SCID mice. (a) Images taken 7, 14, and 28 days after FITC-dextran was injected in the tail vein. New blood vessel formation in cellularized gelatin/microbubble-scaffolds is indicated by FITC-dextran. Scale bar = 100 μm. (b) Cellularized gelatin/microbubble-scaffolds and acellular scaffolds were resected. H&E staining for sections of the paraffin-embedded implanted scaffolds show cell proliferation and blood vessel formation in the scaffolds at day 28 (panel b-i). A section of control acellular scaffold (panel b-ii). (c) Immunohistochemical staining showing the presence of the alveolar epithelial cells SPC-positive type-II pneumocytes and Aqp-5-positive type-I pneumocytes. Cells were counterstained with DAPI.

5. Conclusions

The prevalent challenge in lung tissue engineering today is the lack of adequate vascularization for blood supply during lung tissue regeneration. The current work demonstrates that lung stem/progenitor cells are capable of both differentiating into alveolar epithelial cells and of inducing angiogenesis. We also showed that an alveoli-like gelatin/microbubble-scaffold can support lung stem/progenitor cell proliferation and differentiation as well as angiogenesis. Findings from this study should encourage the use of lung stem/progenitor cells and gelatin scaffolds as models with which to study angiogenesis and pneumocytes proliferation for *in vitro* lung tissue regeneration.

Acknowledgments

We greatly appreciate the service provided by the Flow Cytometric Analyzing and Sorting Core Facility of the First Core Laboratory, College of Medicine, National Taiwan University. We thank Dr. Chiung-Hsiang Cheng for his excellent technical assistance and the Electron Microscopy Core Facility (Department and Graduate Institute of Veterinary Medicine, National Taiwan University, Taipei, Taiwan) for expert assistance. We thank Ms. Chia-Yu, Kuo for her excellent technical assistance in endothelial tube formation assay. This work was supported by research grants from the National Science Council, Taiwan (NSC 100-2321-B-002-048- and 101-2321-B-002-028-) and National Taiwan University Hospital, Taiwan (NTUH-101-059).

Appendix A. Supplementary data

Supplementary data related to this article can be found at http://dx.doi.org/10.1016/j.biomaterials.2014.03.074.

References

[1] Singer HK, Ruchinskas RA, Riley KC, Broshek DK, Barth JT. The psychological impact of end-stage lung disease. Chest 2001;120:1246–52.
[2] Polak JM, Bishop AE. Stem cells and tissue engineering: past, present, and future. Ann N Y Acad Sci 2006;1068:352–66.
[3] Macchiarini P, Jungebluth P, Go T, Asnaghi MA, Rees LE, Cogan TA, et al. Clinical transplantation of a tissue-engineered airway. Lancet 2008;372:2023–30.
[4] Gonfiotti A, Jaus MO, Barale D, Baiguera S, Comin C, Lavorini F, et al. The first tissue-engineered airway transplantation: 5-year follow-up results. Lancet; 2013. pii: S0140-6736: 62033-4.
[5] Herzog EL, Brody AR, Colby TV, Mason R, Williams MC. Knowns and unknowns of the alveolus. Proc Am Thorac Soc 2008;5:778–82.
[6] Lazarus A, Del-Moral PM, Ilovich O, Mishani E, Warburton D, Keshet E. A perfusion-independent role of blood vessels in determining branching stereotypy of lung airways. Development 2011;138:2359–68.
[7] Hislop AA. Airway and blood vessel interaction during lung development. J Anat 2002;201:325–34.
[8] Sugihara H, Toda S, Miyabara S, Fujiyama C, Yonemitsu N. Reconstruction of alveolus-like structure from alveolar type-II epithelial cells in three-dimensional collagen gel matrix culture. Am J Pathol 1993;142:783–92.
[9] Adamson IY, Young L. Alveolar type-II cell growth on a pulmonary endothelial extracellular matrix. Am J Physiol 1996;270:L1017–22.
[10] Cortiella J, Nichols JE, Kojima K, Bonassar LJ, Dargon P, Roy AK, et al. Tissue-engineered lung: an in vivo and in vitro comparison of polyglycolic acid and pluronic F-127 hydrogel/somatic lung progenitor cell constructs to support tissue growth. Tissue Eng 2006;12:1213–25.
[11] Andrade CF, Wong AP, Waddell TK, Keshavjee S, Liu M. Cell-based tissue engineering for lung regeneration. Am J Physiol Lung Cell Mol Physiol 2007;292:L510–8.
[12] Mondrinos MJ, Koutzaki SH, Poblete HM, Crisanti MC, Lelkes PI, Finck CM. In vivo pulmonary tissue engineering: contribution of donor-derived endothelial cells to construct vascularization. Tissue Eng Part A 2008;14:361–8.
[13] Ott HC, Clippinger B, Conrad C, Schuetz C, Pomerantseva I, Ikonomou L, et al. Regeneration and orthotopic transplantation of a bioartificial lung. Nat Med 2010;16:927–33.
[14] Petersen TH, Calle EA, Zhao L, Lee EJ, Gui L, Raredon MB, et al. Tissue-engineered lungs for in vivo implantation. Science 2010;329:538–41.
[15] Cortiella J, Niles J, Cantu A, Brettler A, Pham A, Vargas G, et al. Influence of acellular natural lung matrix on murine embryonic stem cell differentiation and tissue formation. Tissue Eng Part A 2010;16:2565–80.
[16] Auger FA, Gibot L, Lacroix D. The pivotal role of vascularization in tissue engineering. Annu Rev Biomed Eng 2013;15:177–200.
[17] Lin YM, Zhang A, Rippon HJ, Bismarck A, Bishop AE. Tissue engineering of lung: the effect of extracellular matrix on the differentiation of embryonic stem cells to pneumocytes. Tissue Eng Part A 2010;16:1515–26.
[18] Roomans GM. Tissue engineering and the use of stem/progenitor cells for airway epithelium repair. Eur Cell Mater 2010;19:284–99.
[19] Polak DJ. The use of stem cells to repair the injured lung. Br Med Bull 2011;99:189–97.
[20] Wetsel RA, Wang D, Calame DG. Therapeutic potential of lung epithelial progenitor cells derived from embryonic and induced pluripotent stem cells. Annu Rev Med 2011;62:95–105.
[21] Kotton DN. Next-generation regeneration: the hope and hype of lung stem cell research. Am J Respir Crit Care Med 2012;185:1255–60.

[22] Ling TY, Kuo MD, Li CL, Yu AL, Huang YH, Wu TJ, et al. Identification of pulmonary Oct-4+ stem/progenitor cells and demonstration of their susceptibility to SARS coronavirus (SARS-CoV) infection in vitro. Proc Natl Acad Sci U S A 2006;103:9530–5.
[23] Huang CJ, Chien YL, Ling TY, Cho HC, Yu J, Chang YC. The influence of collagen film nanostructure on pulmonary stem cells and collagen-stromal cell interactions. Biomaterials 2010;31:8271–80.
[24] Wang CC, Yang KC, Lin KH, Liu YL, Liu HC, Lin FH. Cartilage regeneration in SCID mice using a highly organized three-dimensional alginate scaffold. Biomaterials 2012;33:120–7.
[25] Ribatti D. Chick embryo chorioallantoic membrane as a useful tool to study angiogenesis. Int Rev Cell Mol Biol 2008;270:181–224.
[26] Radek KA, Kovacs EJ, Gallo RL, DiPietro LA. Acute ethanol exposure disrupts VEGF receptor cell signaling in endothelial cells. Am J Physiol Heart Circ Physiol 2008;295:H174–84.
[27] Park YJ, Repka-Ramirez MS, Naranch K, Velarde A, Clauw D, Baraniuk JN. Nasal lavage concentrations of free hemoglobin as a marker of microepistaxis during nasal provocation testing. Allergy 2002;57:329–35.
[28] Staton CA, Reed MW, Brown NJ. A critical analysis of current in vitro and in vivo angiogenesis assays. Int J Exp Pathol 2009;90:195–221.
[29] Tsao PN, Su YN, Li H, Huang PH, Chien CT, Lai YL, et al. Overexpression of placenta growth factor contributes to the pathogenesis of pulmonary emphysema. Am J Respir Crit Care Med 2004;169:505–11.
[30] Pang C, Gao Z, Yin J, Zhang J, Jia W, Ye J. Macrophage infiltration into adipose tissue may promote angiogenesis for adipose tissue remodeling in obesity. Am J Physiol Endocrinol Metab 2008;295:E313–22.
[31] Nichols JE, Niles JA, Cortiella J. Design and development of tissue engineered lung: progress and challenges. Organogenesis 2009;5:57–61.
[32] Reeh M, Bockhorn M, Görgens D, Vieth M, Hoffmann T, Simon R, et al. Presence of the coxsackievirus and adenovirus receptor (CAR) in human neoplasms: a multitumour array analysis. Br J Cancer 2013;109:1848–58.
[33] Koizumi K. Current surgical strategies for lung cancer with a focus on open thoracotomy and video-assisted thoracic surgery. J Nippon Med Sch 2006;73:116–21.
[34] Nakao S, Kuwano T, Ishibashi T, Kuwano M, Ono M. Synergistic effect of TNF-alpha in soluble VCAM-1-induced angiogenesis through alpha 4 integrins. J Immunol 2003;170:5704–11.
[35] Zhao W, Han Q, Lin H, Sun W, Gao Y, Zhao Y, et al. Human basic fibroblast growth factor fused with Kringle4 peptide binds to a fibrin scaffold and enhances angiogenesis. Tissue Eng Part A 2009;15:991–8.
[36] Stenmark KR, Abman SH. Lung vascular development: implications for the pathogenesis of bronchopulmonary dysplasia. Annu Rev Physiol 2005;67:623–61.
[37] White AC, Lavine KJ, Ornitz DM. FGF9 and SHH regulate mesenchymal Vegfa expression and development of the pulmonary capillary network. Development 2007;134:3743–52.
[38] Grainger SJ, Carrion B, Ceccarelli J, Putnam AJ. Stromal cell identity influences the in vivo functionality of engineered capillary networks formed by co-delivery of endothelial cells and stromal cells. Tissue Eng Part A 2013;19:1209–22.
[39] Mura M, Binnie M, Han B, Li C, Andrade CF, Shiozaki A, et al. Functions of type-II pneumocyte-derived vascular endothelial growth factor in alveolar structure, acute inflammation, and vascular permeability. Am J Pathol 2010 Apr;176(4):1725–34.
[40] Chung KY, Mishra NC, Wang CC, Lin FH, Lin KH. Fabricating scaffolds by microfluidics. Biomicrofluidics 2009;3:22403.
[41] Neuss S, Apel C, Buttler P, Denecke B, Dhanasingh A, Ding X, et al. Assessment of stem cell/biomaterial combinations for stem cell-based tissue engineering. Biomaterials 2008;29:302–13.
[42] Yu J, Gu Y, Du KT, Mihardja S, Sievers RE, Lee RJ. The effect of injected RGD modified alginate on angiogenesis and left ventricular function in a chronic rat infarct model. Biomaterials 2009;30:751–6.
[43] Shachar M, Tsur-Gang O, Dvir T, Leor J, Cohen S. The effect of immobilized RGD peptide in alginate scaffolds on cardiac tissue engineering. Acta Biomater 2011;7:152–62.
[44] Sun YS, Peng SW, Lin KH, Cheng JY. Electrotaxis of lung cancer cells in ordered three-dimensional scaffolds. Biomicrofluidics 2012;6. 14102-14111-14.
[45] Cavalcante FS, Ito S, Brewer K, Sakai H, Alencar AM, Almeida MP, et al. Mechanical interactions between collagen and proteoglycans: implications for the stability of lung tissue. J Appl Physiol 1985;2005(98):672–9.
[46] Namati E, Thiesse J, de Ryk J, McLennan G. Alveolar dynamics during respiration: are the pores of Kohn a pathway to recruitment? Am J Respir Cell Mol Biol 2008;38:572–8.

Please cite this article in press as: Ling T-Y, et al., Differentiation of lung stem/progenitor cells into alveolar pneumocytes and induction of angiogenesis within a 3D gelatin – Microbubble scaffold, Biomaterials (2014), http://dx.doi.org/10.1016/j.biomaterials.2014.03.074